Antiviral Research 96 (2012) 115–126

Contents lists available at SciVerse ScienceDirect

Antiviral Research

journal homepage: www.elsevier.com/locate/antiviral

Review

Structural biology of dengue virus enzymes: Towards rational design of therapeutics

Christian G. Noble *, Pei-Yong Shi *

Novartis Institute for Tropical Diseases, 10 Biopolis Road, #05-01 Chromos, Singapore 138670, Singapore

ARTICLE INFO

Article history:
Received 17 July 2012
Revised 3 September 2012
Accepted 7 September 2012
Available online 17 September 2012

Keywords:
Flavivirus
Dengue virus
Enzyme
Crystal structure
Structure-based design

ABSTRACT

Development of anti-dengue therapy represents an urgent un-met medical need. Towards antiviral therapy, recent advances in crystal structures of DENV enzymes have led to the possibility of structure-based rational design of inhibitors for anti-dengue therapy. These include (i) the structure of the 'active' form of the DENV protease in complex with a peptide substrate; (ii) the structure of DENV methyltransferase bound to an inhibitor that selectively suppresses viral methyltransferase, but not human methyltransferases; (iii) the structure of DENV RNA-dependent RNA polymerase in complex with a small-molecule compound. This review summarizes the structural biology of these three key enzymes (protease, methyltransferase, and polymerase) that are essential for DENV replication. The new structural information has provided new avenues for development of anti-dengue therapy.

Contents

1. Introduction

Dengue is the most prevalent mosquito-borne viral disease and there are currently no approved antivirals or vaccines. Upon DENV infection, some individuals develop mild disease with flu-like symptoms, whereas a few individuals develop severe disease – dengue hemorrhagic fever (DHF) and dengue shock syndrome (DSS). DHF and DSS can be fatal without supportive medical treatment (Simmons et al., 2012). Three major approaches are being pursued to control DENV infections. (i) Mosquito control is currently the most effective means to reduce human cases of DENV infection. (ii) Dengue vaccines are in various stages of clinical trials, but none have been approved for clinical use. (iii) Antiviral therapy remains to be developed for the treatment of DENV infection. The combination of vector control, vaccination, and antiviral therapy will provide a complementary solution to minimize the dengue disease burden.

The family *Flaviviridae* includes three genera, flavivirus, pestivirus, and hepaciviruses. DENV is a member of the genus flavivirus, which includes a number of important human pathogens. These include West Nile virus (WNV), yellow fever virus (YFV), tick-borne encephalitis virus (TBEV), and Murray Valley encephalitis virus (MVEV). The viral genome is a single-stranded RNA that is approximately 11 kb of positive sense. The RNA encodes three structural proteins (capsid, envelope, and membrane) that form the virus particle and eight non-structural proteins (NS1, NS2A, NS2B, NS3, NS4A, 2K peptide, NS4B, and NS5) that are required for replication of the virus (Bollati et al., 2010). The only known enzymes are encoded by NS3 and NS5, both of which catalyze multiple different activities (Lescar et al., 2008; Malet et al., 2008). The N-terminal domain of NS3 is a protease (with NS2B as a cofactor) and the C-terminal domain is an RNA helicase. NS5 contains a methyltransferase (MTase) at the N terminus and an RNA-dependent RNA polymerase (RdRp) at the C terminus.

* Corresponding authors. Tel.: +65 67222920; fax: +65 67222916 (C.G. Noble), tel.: +65 67222909; fax: +65 67222916 (P.-Y. Shi).
E-mail addresses: christian.noble@novartis.com (C.G. Noble), pei_yong.shi@novartis.com (P.-Y. Shi).

0166-3542/$ - see front matter © 2012 Elsevier B.V. All rights reserved.
http://dx.doi.org/10.1016/j.antiviral.2012.09.007

A number of strategies have been pursued for developing anti-DENV therapy (Noble et al., 2010). Direct-acting antiviral (DAA) molecules have been identified through cell-based approaches (e.g., virus infection or replicon cell line screens) (Xie et al., 2011) or target-based approaches (e.g., screening biochemical enzyme assays or structure-based rational design) (Lim et al., 2011; Niyomrattanakit et al., 2010). In this communication, we review the recent advances in structure-based design of small-molecule inhibitors targeting three key DENV enzymes, protease, MTase, and RdRp.

2. DENV protease

DENV protease is located in the N terminus of the NS3 protein. It is a typical serine protease containing a catalytic triad of His51, Asp75, and Ser135. The flavivirus protease requires a stretch of approximately 40 amino acids from the cytosolic domain of NS2B for catalytic activity (Falgout et al., 1991). NS2B is predicted to contain three transmembrane helices. The viral genome is expressed as a long polyprotein that must be cleaved into the individual proteins for the virus to replicate (Valle and Falgout, 1998). The viral protease is required to cleave the junctions between C-prM, NS2A–NS2B, NS2B–NS3, NS3–NS4A, NS4A-2K peptide, and NS4B–NS5, whilst host signal peptidases in the ER lumen cleave the junctions of the pr-M, M-E, E-NS1, NS1–NS2A, and 2K peptide-NS4B (Fig. 1). Antiviral drugs have been approved for other viral proteases, including recently for the hepatitis C virus (HCV) protease (Venkatraman, 2012), a virus within the same family as DENV.

For rational design of DENV-protease inhibitors, it is critical to have a crystal structure of the DENV protease in a catalytically-competent conformation. Several crystal structures have been solved for flavivirus proteases in the absence of additional ligands. These include DENV-1 and DENV-2, a WNV active-site mutant, as well as MVEV protease in the context of the full-length NS3 protein (Aleshin et al., 2007; Chandramouli et al., 2010; Erbel et al., 2006; Assenberg et al., 2009). These structures all contained the ~40 amino-acid region of NS2B that is required for catalytic activity in vitro. In agreement with the requirement of NS2B for protease activity, one β strand of DENV NS2B (residues 51–57) forms part of the core structure of NS3 protease. This strand is important for stabilizing the NS3 protease domain and enhancing its solubility in vitro (Erbel et al., 2006). The remainder of NS2B adopts different conformations in DENV-1, DENV-2, and WNV proteases (Fig. 2A) (Erbel et al., 2006; Chandramouli et al., 2010; Aleshin et al., 2007); the same region of NS2B is largely disordered in MVEV protease (Assenberg et al., 2009). These structures showed that the rest of NS2B is flexible and is disordered in the absence of an additional ligand.

Structures have also been determined for complexes of ligands bound to the WNV protease. These include two different peptide-based inhibitors (Erbel et al., 2006; Robin et al., 2009) and the broad-spectrum serine-protease inhibitor, aprotinin (Aleshin et al., 2007). In these structures, the rest of NS2B becomes ordered and it folds into a β hairpin that wraps around NS3, forming part of the S2 and S3 pockets of the active site. These structures showed that NS2B becomes ordered upon binding to a substrate and explained why a large stretch of NS2B was required for catalytic activity in vitro. We will refer to this conformation as 'closed' and the conformation in which part of NS2B is away from the active site as the 'open' conformation.

In the absence of a crystal structure of the 'closed' conformation of DENV protease, anti-DENV protease efforts were guided by *in silico* modeling using the WNV structures (Knehans et al., 2011; Wichapong et al., 2010). Recently, crystal structures of a peptide inhibitor and of aprotinin bound to the DENV-3 protease were solved (Noble et al., 2012). The structure of the peptide bound to the protease finally showed that the DENV protease also forms the same 'closed' conformation seen in the WNV protease, with the flexible region of NS2B forming a β hairpin that wraps around the NS3 core of the protease (Fig. 2B). In contrast to the WNV protease–aprotinin structure (Aleshin et al., 2007), the DENV-3 protease–aprotinin structure showed that NS2B did not adopt the 'closed' conformation (Noble et al., 2012). The latter result indicates that, at least in the case of the DENV protease, interactions between aprotinin and the flexible β hairpin of NS2B are not required for inhibition of the protease by aprotinin. This observation may in part explain why aprotinin is about 10 times more potent in DENV protease than WNV protease (Mueller et al., 2007).

WNV and DENV proteases have high sequence conservation (41% amino-acid identity within the protease region of NS3). NS2B is the most divergent between the two viruses (only 19% identity), particularly within the β hairpin (about 10% identity). Despite the high sequence conservation, WNV and DENV proteases have different sequence preferences in their cleavage sites. Peptide profiling for DENV-2 protease showed that it had a sequence preference at P3 for K > R, at P2 for R > K, and at P1 for R > K (Li et al., 2005). This is different from WNV protease where the preferred P2 residue is K > R (Shiryaev et al., 2007a). The difference in the preference at the P2 residue is due to Asn84 in WNV protease, which is Thr83 in DENV-3 protease and Ser83 in DENV-2 protease. Mutation of Asn84 to Ser in WNV protease decreased the K_m (increased the affinity) for a substrate containing Arg at P2 over a substrate containing Lys at this position (Chappell et al., 2006). An explanation for this can now be seen from the DENV-3 crystal structure, which clearly shows that the shape of the S2 pocket in WNV protease is narrower than that in DENV protease (Fig. 2C).

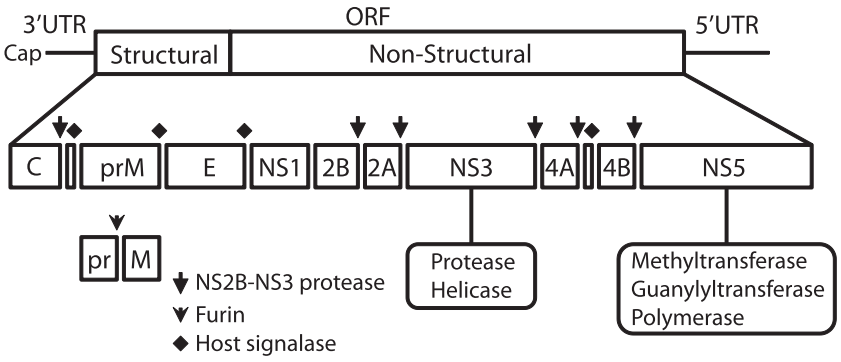

Fig. 1. Organization of the DENV genome. The genome is translated into a single polyprotein that is post-translationally cleaved into the individual proteins by a combination of host proteases and the DENV NS2B–NS3 protease. The sites of cleavage by known proteases are indicated.

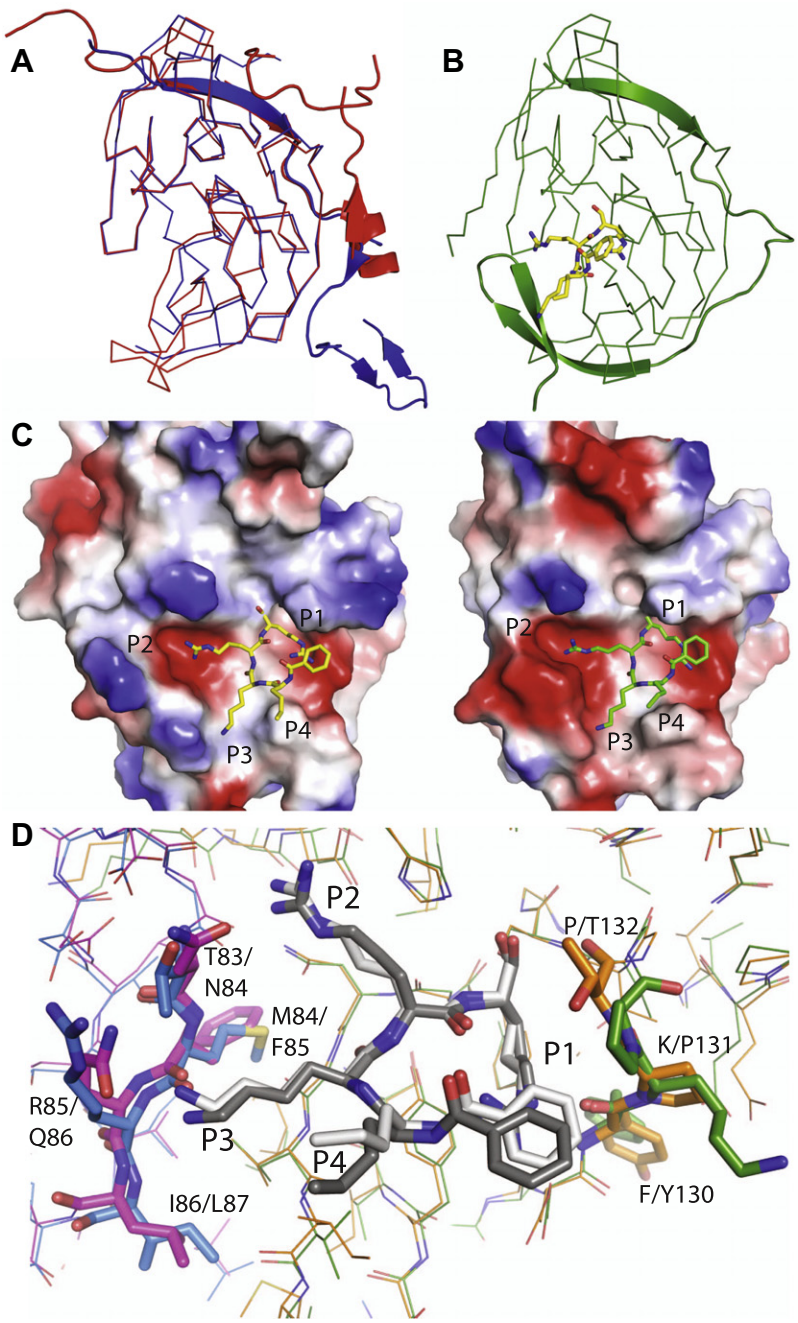

Fig. 2. Comparison of DENV and WNV protease structures. (A) The crystal structures of the proteases from DENV-1 (PDB ID: 3L6P; blue) and DENV-2 (PDB ID: 2FOM; red). NS2B is shown as a cartoon and NS3 as a ribbon. (B) The crystal structure of the protease DENV-3 (PDB ID: 3U1I; green), shown in the same orientation and format as (A). The peptide bound to DENV-3 protease is shown as yellow sticks. (C) Crystal structures of DENV protease (PDB ID: 3U1I; left) and WNV protease (PDB ID: 2FP7; right) are shown in surface representation and colored according to their electrostatic potential. Positive potential is blue and negative potential is red. (D) Residues shown to affect the specificity of the S2–S3 and S1′–S2′ pockets are shown as sticks and the amino acids are labeled. WNV protease NS2B is pink and NS3 is orange. DENV protease NS2B is blue and NS3 is green. The peptide is grey with the ligand bound to DENV protease shown in a darker shade. For each labeled amino acid, residue identity and numbering, where different, are indicated for DENV first and for WNV second.

The P1 Arg sidechain is 5.6 Å from Thr83 in the DENV-3 protease compared to 3.6 Å to Asn84 in the WNV protease.

Another difference in the substrate-binding site is the electrostatic potential of the S2 and S3 pockets, which are largely formed by NS2B (Fig. 2C, where red is negative electrostatic potential and blue is positive). The DENV-3 protease has Arg85 of NS2B near the S3 pocket. Since this is positively charged, it points away from the P3 lysine (Noble et al., 2012). The only interaction that the P3 residue makes in the DENV-3 protease is to the backbone carbonyl of Met84. WNV protease has Gln86 instead of Arg85, which forms a charge-reinforced hydrogen bond with the P3 Lys (Erbel et al., 2006). It is surprising that there is still a strong preference for a charged basic residue at this position for either WNV or DENV proteases (Li et al., 2005; Shiryaev et al., 2007a), most likely because the P3 Lys forms charge-reinforced hydrogen bond(s) with the β hairpin of NS2B, contributing to the stabilization of the 'closed' conformation.

Another notable difference in the sequence specificity of the DENV and WNV proteases is on the prime side of the substrate-binding site. DENV protease prefers Ser at P1′ and has little

sequence specificity at P2′, whilst WNV protease prefers Gly at both P1′ and P2′ (Shiryaev et al., 2007a; Lim et al., 2008). A comparison of the structures of WNV and DENV-3 proteases bound to the same peptide suggests that the difference in the sequence specificity at the S1′ and S2′ pockets is due to a structural difference in the helical turn between the S1′ and S2′ pockets (Fig. 2D). DENV protease contains Lys131 and Pro132 on this helical turn; whereas WNV protease has very different side chains, Pro and Thr at the same positions. Mutagenesis of both residues in the WNV protease to the DENV sequence changes the sequence preference at P1′ and P2′ to be more like that of DENV protease (Shiryaev et al., 2007a). The crystal structure of the DENV-3 protease shows that these residues cause a deviation in the conformation of the protein backbone between WNV and DENV proteases and consequently changes the shapes of the S1′ and S2′ pockets.

The new structures of the DENV-3 protease are very similar to the WNV protease (RMSD is 0.6 Å), but the enzymes have very different catalytic properties in vitro. The catalytic efficiency of DENV protease (k_{cat}/K_m) is 2–50 times lower than WNV protease on the same substrates (Shiryaev et al., 2007b; Mueller et al., 2007). It is therefore surprising that the structures are not more divergent. The WNV protease typically has more than ten times greater catalytic efficiency than DENV-2 protease (Schuller et al., 2011). The WNV protease is also much more susceptible to inhibition by small peptide inhibitors. A series of di- and tri-peptide aldehydes were on average over 110 times more potent against WNV protease than DENV-2 protease (Schuller et al., 2011). The reason for this may simply be due to the different affinities of the peptides for the DENV versus the WNV proteases. It has been shown by NMR that the NS2B β hairpin is predominantly bound to NS3 in the 'closed' conformation in the WNV protease, but in the DENV-2 protease the β hairpin is largely 'open' (Wu et al., 2007; de la Cruz et al., 2011; Su et al., 2009). Any peptides that have the P2 and P3 residues must stabilize the 'closed' conformation of the protease in order to bind to it. Since a greater proportion of DENV-2 protease is 'open' (Wu et al., 2007; de la Cruz et al., 2011; Su et al., 2009), it is reasonable to assume that less energy is required to stabilize the 'closed' conformation in the WNV protease (i.e., there is less entropic penalty associated with peptide binding). This would explain the different potencies seen for the di- and tri-peptides. However, it is not known whether the same 'open' trend is true inside the cell. It may be that in the context of the replication complex, the DENV protease is always in the 'closed' conformation.

To date there are no co-crystal structures of the DENV protease bound to non-peptidic inhibitors identified through high-throughput screening (HTS). Several non-peptidic small-molecule inhibitors of DENV protease have been identified (for example (Bodenreider et al., 2009; Tomlinson and Watowich, 2012; Tomlinson et al., 2009), but due to space constraints and lessons from small-molecule development for HCV protease, we will only discuss peptide-based inhibitors here. HCV protease is an equally challenging antiviral target and the first antivirals approved for clinical use against HCV genotype 1 are derived from peptide-based inhibitors, that were discovered through rational structure-based design (Venkatraman, 2012). It is likely that small-molecule inhibitors of DENV protease could also be rationally derived from peptidic inhibitors using multiple ligand-bound crystal structures. Detailed SAR (structure–activity relationship) studies of small peptide-aldehyde inhibitors of DENV protease suggest that the preferred amino acids KRR can be replaced one at a time, retaining activity and reducing the overall positive charge of the inhibitors (Yin et al., 2006a). The amino-terminal capping group on peptide aldehydes also influences their activity (Schuller et al., 2011). Similar tripeptide aldehydes have been shown to inhibit WNV replication in cell culture, showing that this is a valid antiviral approach (Stoermer et al., 2008). However, generating potent inhibitors against the DENV protease in vitro requires electrophilic warheads that form covalent bonds with the active-site serine, with boronic acid being the most potent (Yin et al., 2006b). Recently, di- and tri-retro-peptide inhibitors (in which the N and C termini are reversed) have been developed; these peptide inhibitors lack an electrophilic warhead and still inhibit DENV protease in vitro with low micromolar potency (Nitsche et al., 2012). These compounds contain aromatic groups in addition to the retro peptide and may represent a starting point for rational structure-based design; further progress of this approach requires co-crystal structures to understand how these compounds bind to the DENV protease.

3. DENV MTase

NS5 is the largest flavivirus protein and also the most highly conserved with approximately 67% amino-acid identity between DENV serotypes 1–4. MTase is located in the N terminus of NS5 (Bollati et al., 2010). Flavivirus MTase methylates the 5′ RNA cap (Ray et al., 2006). WNV and DENV MTases were also recently shown to perform internal RNA methylation (Dong et al., 2012).

The 5′ terminus of flavivirus genomic RNA has a type 1 cap structure (m^7GpppAm). This cap structure contains a guanine nucleotide attached to the first nucleotide (adenosine) of the RNA via a 5′–5′ triphosphate linker. A type 1 cap is methylated at the N-7 position of the guanine (m^7G), as well as on the 2′ OH of the ribose of the first nucleotide (Am) of the RNA. Three enzymatic steps are required to form the flavivirus cap structure. First, the triphosphate at the 5′ end of the RNA (pppA-RNA) is hydrolyzed to generate ppA-RNA. This reaction is catalyzed by the NS3 RNA triphosphatase (Wengler et al., 1985). Secondly, a guanylyl transferase (GTase) transfers the GMP moiety from GTP onto the 5′ end of the ppA-RNA to form a 5′–5′ triphosphate linkage, generating GpppA-RNA. The GTase reaction was assumed to occur via a covalent intermediate between GMP and a Lys residue on the enzyme (Ghosh and Lima, 2010). The flavivirus GTase has not been conclusively identified, but this activity is proposed to reside in the MTase domain of NS5 (Bollati et al., 2009; Egloff et al., 2007; Issur et al., 2009). Thirdly, the GpppA-RNA is then methylated at both the N-7 and 2′-*O* positions of the cap structure, leading to m^7GpppAm-RNA. Flavivirus MTase catalyzes the two cap methylations in a sequential manner with N-7 methylation preceding the 2′-*O* methylation, i.e., GpppA-RNA → m^7GpppA-RNA → m^7GpppAm-RNA (Dong et al., 2010a). Both methylations use *S*-adenosyl methionine (SAM) as the methyl donor, generating the by-product *S*-adenosyl homocysteine (SAH). The fact that the flavivirus MTase and RdRp domains are physically linked within a single NS5 protein suggests that RNA-cap formation is coupled to viral RNA replication (Dong et al., 2008b).

The flavivirus MTase requires distinct viral RNA-structural and -sequence elements for the two RNA-cap methylations. Both DENV and WNV N-7 methylations require stem–loop RNA structures with the specific 5′-viral-RNA sequence (Dong et al., 2010a, 2007; Ray et al., 2006). For 2′-*O* methylation, WNV MTase requires the first 20 nucleotides of the genomic RNA, whereas DENV 2′-*O* MTase requires capped RNA with only 6 nucleotides (m^7GpppACCCCC) (Egloff et al., 2002). It remains to be determined whether DENV MTase performs 2′-*O* methylation more efficiently on an authentic viral-RNA substrate than on a non-viral sequence, such as m^7GpppACCCCC. For both WNV and DENV 2′-*O* methylation, RNA substrates that are N-7 methylated (m^7GpppA-RNA) are much more efficient substrates than RNA without N-7 methylation (GpppA-RNA) (Dong et al., 2007).

Mutagenesis of residues within WNV and DENV MTase showed that N-7 methylation enhances viral RNA translation; mutant viruses defective in N-7 methylation are lethal, indicating that N-

7 methylation is a potential antiviral target. In contrast, mutant WNV and DENV defective in 2′-*O* methylation are replication competent in Vero and BHK cells (both cells are defective in interferon production) (Dong et al., 2010a, 2008a). It was recently found that the function of 2′-*O* methylation of the viral RNA cap is to evade the host innate immune response by mimicking a host mRNA, which all contain the identical 5′ type I cap (Daffis et al., 2010). These results suggest that inhibitors against flavivirus 2′-*O* methylation would not directly suppress viral replication, but they suggest that viral RNA without 2′-*O* methylation would be eliminated by the host innate immune response.

Numerous crystal structures have now been determined for the flavivirus MTases from multiple different viruses (reviewed in Bollati et al. (2010)), including structures with various cap analogs. All structures of flavivirus MTases adopt very similar conformations with an RMSD between different viruses of <1 Å, and high sequence conservation. The MTases consist of a core domain of seven β strands, surrounded by four α helices. This core is encircled by N- and C-terminal extensions, which wrap around the core fold. The N-terminal extension has a helix-turn-helix followed by a β strand and an α helix; the C-terminal extension consists of an α helix and two β strands. Within the core domain is a binding site for the methyl donor of the methylation reaction, SAM (Fig. 3). There is also a pocket that binds to GTP and the guanine moiety of the RNA cap, referred to as the GTP pocket. This pocket is formed between the core domain and the N-terminal extension and mutagenesis of residues lining this pocket suggests that it is functionally more important for 2′-*O* activity than for N-7 activity (Dong et al., 2008a), indicating that the m^7G of the capped RNA binds here during 2′-*O* methylation. The GTP pocket has been referred to as the higher-affinity binding site (Bollati et al., 2010).

Several crystal structures have been determined bound to multiple different cap analogs (Bollati et al., 2009; Egloff et al., 2007; Geiss et al., 2009; Assenberg et al., 2007). The guanine base from very different cap analogs including GpppG, GpppA, m^7GpppA, m^7GpppAm and m^7GpppGm always binds to the GTP pocket, by stacking against Phe25 (numbered according to DENV MTase).

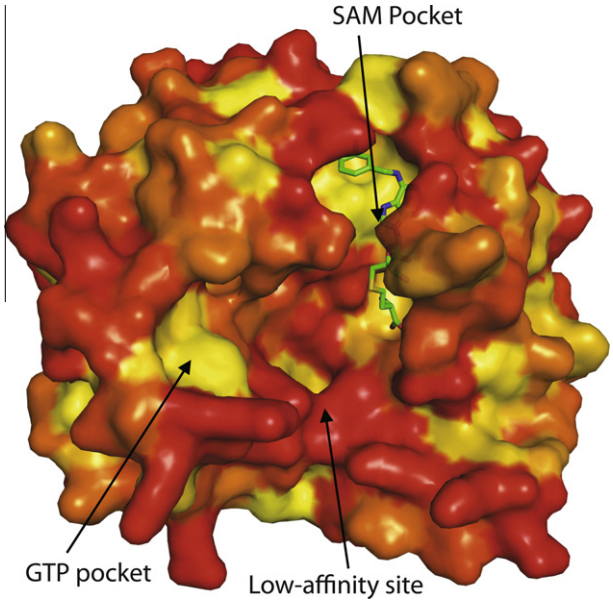

Fig. 3. Hydrophobicity of the DENV MTase. The crystal structure of DENV-3 MTase bound to compound 10 (PDB ID: 3P8Z) (Lim et al., 2011). The structure is shown in surface representation and amino acids are colored in a scale according to their hydrophobicity, where red is polar and yellow is hydrophobic. Ligand-binding pockets are indicated.

Binding is also stabilized by interactions between the ribose 2′-OH and Lys14 and Asn18, and between the α phosphate and Ser213 and Lys29 (Egloff et al., 2007; Geiss et al., 2009). Guanine is distinguished in this site over adenine by the N2 of guanine forming hydrogen bonds with backbone carbonyls of Leu17 and Leu20 (Egloff et al., 2002). There are no interactions with the N-7 methyl group, explaining why m^7GpppA and GpppA both bind to DENV MTase (Egloff et al., 2007). It is not clear from the crystal structures why 2′-*O* methylation is more efficient on N-7-methylated, capped RNA (Dong et al., 2010a). The second nucleotide (the nucleoside immediately following the triphosphates) adopts multiple different conformations, indicating that there is less affinity for this nucleotide. In many structures, the second nucleotide adopts a stacked conformation where its base stacks on the m^7G (Egloff et al., 2007; Geiss et al., 2009). However, these conformations are unlikely to be relevant for methyltransferase catalysis, since the cap analog is far away from the SAM-binding site. In other crystal structures, the cap analog adopts an extended conformation where the triphosphate points towards the SAM-binding site, but the second nucleotide is disordered (Assenberg et al., 2007; Bollati et al., 2009; Egloff et al., 2007; Geiss et al., 2009). It was noted that this conformation is more commonly found in crystal structures produced in lower ionic strength (Geiss et al., 2009), indicating that the stacked conformations may be a crystallographic artifact.

In the crystal structure of Wesselsbron virus MTase bound to GMP, the GMP was found to bind to the GTP pocket via a covalent bond between Lys28 and the α phosphate (Bollati et al., 2009). However, during further assays in vitro it was not possible to transfer the GMP group to diphosphate-RNA. A Lys residue is normally essential for GTase activity (Ghosh and Lima, 2010), but Lys28 is not strictly conserved in flavivirus MTases and is commonly replaced by Arg (Bollati et al., 2009), so it is still not clear whether the N-terminal domain of NS5 is a true GTase, although it was speculated that Arg may also form a covalent intermediate (Bollati et al., 2009). Mutagenesis of the equivalent residue in DENV MTase, Lys29, reduced but did not abolish the ability of the enzyme to form a covalent intermediate with GMP, and Lys30 was suggested to substitute for the active-site Lys in this mutant (Issur et al., 2009). Subsequent assays suggested that DENV MTase transfers GMP onto a diphosphate-RNA substrate, indicating that it does have GTase activity in vitro (Issur et al., 2009). However, this activity has not been shown for MTases that have Arg-Arg and no Lys at these positions, suggesting that the covalent intermediate may be an in vitro artifact caused by GTP binding. Furthermore, GTases should specifically use GTP (not ATP, CTP, or UTP) as a substrate to form the covalent GMP–enzyme complex. Our unpublished results showed that both DENV and WNV MTases could non-specifically form covalent complexes upon incubation with GTP, ATP, CTP, or UTP. Overall, it remains to be experimentally demonstrated whether flavivirus MTase functions as a GTase.

The GTP-binding pocket may be a valid site for the design of direct-acting antivirals. Binding assays have been developed, based on the displacement of a fluorescent GTP analog bound to this site that can be used for HTS (Geiss et al., 2011; Stahla-Beek et al., 2012). This approach has identified compounds that inhibit the in vitro guanylyltransferase activity of DENV MTase with low micromolar potency. One compound, BG-323, also showed inhibition in the DENV replicon (Stahla-Beek et al., 2012). This compound has yet to be tested on DENV MTase activity since it would be expected to also inhibit 2′-*O* activity, if the compound is binding to the GTP pocket. This compound may represent a valid starting point for structure-based optimization.

Other structures with capped RNA analogs, as well as the surface electrostatic potential suggest that there is a second lower-affinity binding site between the SAM and GTP pockets that binds

RNA (Fig. 3) (Assenberg et al., 2007). This region is highly positively charged in flavivirus MTases and frequently bound by sulfates and phosphates in crystal structures, indicating that it is the RNA-binding site. This lower-affinity site is formed by the core domain and by a channel between two helices of the N-terminal extension. Since the same enzyme performs two very distinct methylation reactions, and it only contains a single binding site for SAM, it is very likely that the RNA substrate must reposition between the two methylations (Dong et al., 2008a). N-7 methylation precedes 2′-*O* and requires a stem loop, so it is thought that the capped RNA, including the stem loop binds in the lower-affinity site and the guanine of the cap is presented to the SAM methyl donor for N-7 methylation. The RNA substrate then slides further into the MTase so that the m^7G enters the higher-affinity site (i.e., GTP pocket) and the ribose of the first nucleotide is now correctly positioned for methylation at the 2′-OH. It is not known how many MTases are required for this reaction. Combining mutants that are inactive in either 2′-*O* or N-7 activity produces a type 1 methylated cap, indicating that the activity can be performed in trans, so it is possible that one MTase enzyme bound to SAM would perform a single N-7 or 2′-*O* methylation event during the production of each cap structure (Dong et al., 2008a).

Recently the first complex of a flavivirus MTase with RNA was determined (Yap et al., 2010). The RNA was bound to two MTase molecules out of four in the asymmetric unit and the RNA was stabilized in the crystal by forming a kissing loop. However, the RNA-binding mode was likely a crystallization artifact. Despite the large number of crystal structures of flavivirus MTases bound to 5′-RNA-cap analogs, there is still no structure of a complex of the MTase with a capped RNA in a competent conformation for catalyzing methyl transfer. A model for a short-capped RNA bound to the lower-affinity binding site where it would need to be held for N-7 methyl transfer suggests that it would be held weakly by electrostatic interactions (Milani et al., 2009), highlighting the difficulty in obtaining a structure of this complex.

The flavivirus MTase is an obvious target for the development of antiviral compounds since it contains well defined ligand-binding pockets (Fig. 3). The structures of DENV MTase bound to ribavirin shows how a ligand bound to this pocket would inhibit binding by the RNA cap (Benarroch et al., 2004). Another inhibitor, aurintricarboxylic acid (Fig. 4), was identified by high-throughput docking using the structure of the Wesselsbron virus MTase and found to inhibit the 2′-*O* activity of DENV MTase with an IC_{50} of about 2 μM (Milani et al., 2009). The compound was predicted to bind to the lower-affinity site, although this has not been shown experimentally. Crystal structures of flavivirus MTases bound to the natural product, sinefungin, have been determined for Wesselsbron virus and West Nile virus MTases (Bollati et al., 2009; Dong et al., 2010b). Sinefungin contains a carbon and amine in place of the methylated sulfur in SAM (Fig. 4). This amine would be charged at physiological pH and mimics the charged methyl-sulfur. However, the crystal structures show that this ligand does not pick up any additional interactions with the protein in the absence of the methylation substrate. Nevertheless, these results demonstrate that the flavivirus MTase is capable of binding other ligands in the SAM site.

Recent studies have identified a conserved cavity in the flavivirus MTase that is next to the adenine base of the SAM-binding site (Dong et al., 2010b; Lim et al., 2011). This pocket is largely hydrophobic and is not present in crystal structures of unrelated methyltransferases that have been determined. By rationally designing compounds based on the product of the methylation reaction, it is possible to target this site to develop inhibitors that are potent against the DENV MTase, but do not inhibit human RNA or DNA MTases in vitro (Lim et al., 2011). Since the pocket is hydrophobic, lipophilic groups can be attached to the adenine base of the SAM to

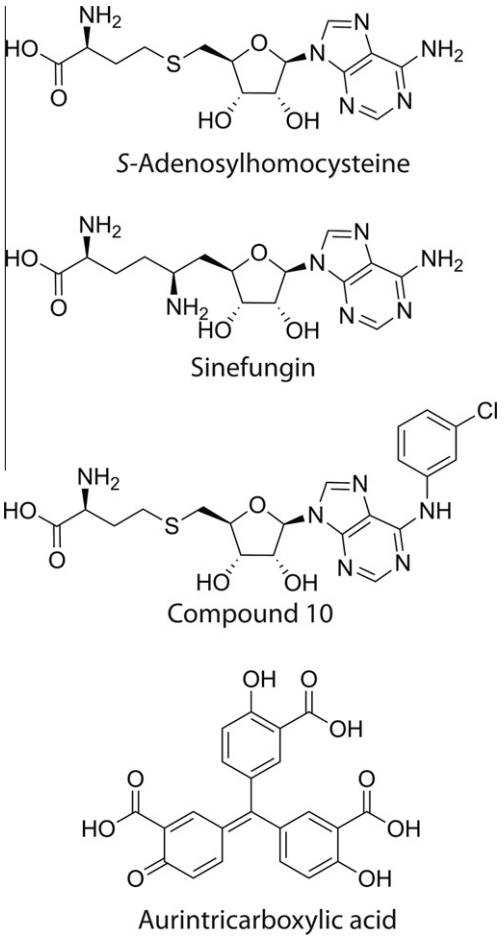

Fig. 4. Structures of compounds that inhibit the activity of DENV MTase in vitro.

increase the potency of inhibitors against the enzyme. Compared with SAH (Fig. 4), compound 10 contained an N-6 benzyl substituent and exhibited improved potencies against DENV N-7 and 2′-*O* methylations; more importantly, this compound no longer inhibits human RNA and DNA MTase activities. The crystal structure of DENV MTase in complex with compound 10 shows that the N6 benzyl ring fits snugly into the hydrophobic pocket and displaces Phe133 from the pocket, effectively changing the size and shape of the pocket (Lim et al., 2011). These results proved the concept that selective inhibitors could be designed by targeting compounds to structural features unique to the disease-related MTase.

Most structures of flavivirus MTases have been solved with a ligand bound to the SAM site. The obvious exception is the Modoc virus MTase, which was solved both bound to SAM and without any ligand (Jansson et al., 2009). In all other structures SAM or SAH remains bound to the recombinant MTase during the purification process. When DENV MTase is expressed and purified from *Escherichia coli*, the enzyme remains tightly bound to SAM during purification (Lim et al., 2011), but this degrades to the product of the methylation reaction, SAH over time. Recent structures with different ligands bound to this site indicate that the endogenous SAM/SAH can be competed out (Bollati et al., 2009; Dong et al., 2010b; Lim et al., 2011). However, attempts to mutate key residues within the SAM pocket in DENV MTase in an attempt to produce an unbound DENV MTase that still crystallizes have been unsuccessful (unpublished results). Mutation of Asp79 that co-ordinates two water molecules mediating interactions with the zwitterionic amino-acid region of SAM, result in an unstable enzyme that is poorly expressed and largely insoluble. This result suggests that the DENV

MTase is unstable in the absence of a ligand at this site. Crystals of DENV MTase soaked with the cap analog, m7GpppG, lost the SAH ligand (Egloff et al., 2007). There was no large conformation change on loss of the ligand and it is likely that the protein was stabilized by crystal-packing interactions. The fact that the DENV MTase remains tightly bound to SAM makes a rational structure-based-design program more challenging since compounds must outcompete a high-affinity endogenous ligand in vivo that is at high concentration. Whilst this does not prevent the design of antivirals targeting this site, it may be difficult to develop an orally bioavailable drug with this mechanism of action.

4. DENV RdRp

Flavivirus RdRp, located in the C terminus of the NS5 protein, is essential for viral replication. The RdRp is likely to be the best target for developing direct-acting antivirals that target all four serotypes of DENV (Rawlinson et al., 2006). Viral polymerases have been clinically validated as the target of both nucleoside and non-nucleoside inhibitors. Nucleosides are the most widely used class of marketed antivirals and act by terminating the extending RNA chain during RNA replication. They also provide the greatest barrier to resistance (Yin et al., 2009b). Before a nucleoside can terminate a viral RNA chain, it needs to penetrate into the cell, be converted to its triphosphate derivative, recognized by the viral polymerase, and incorporated into the viral RNA chain. Therefore, nucleosides have complex and unpredictable SAR (Noble et al., 2010). By contrast, non-nucleoside inhibitors act by allosterically blocking polymerase activity, and often bind directly to the polymerase so can be improved by rational structure-based design.

In infected cells, the DENV RdRp first synthesizes a complementary negative-sense RNA and forms a double-stranded RNA intermediate. The negative strand then acts as a template for production of the positive-sense RNA genome. Approximately 10–100 times more positive sense RNA is made and all the negative sense RNA exists as a double-stranded intermediate (Chu and Westaway, 1985). In vitro assays using purified recombinant NS5 showed that it could replicate a negative sense RNA from a positive sense subgenomic RNA template containing both the 5′ and 3′ ends of the viral genome (Ackermann and Padmanabhan, 2001). This showed that NS5 is capable of de novo RNA synthesis in the absence of an RNA primer. This means the polymerase must bind to a viral RNA template as well as two free NTPs to catalyze formation of a nascent phosphodiester bond between them. NS5 also synthesized an RNA that was double the size, presumably through a 'copy back' mechanism (You and Padmanabhan, 1999). The relative amount of these two products is temperature dependent; the initiation phase is temperature dependent, while elongation is not (Ackermann and Padmanabhan, 2001). Based on these data, it was proposed that the DENV RdRp undergoes a conformational change from a 'closed' initiation complex bound to single-stranded RNA to an 'open' elongation complex bound to double-stranded RNA (Ackermann and Padmanabhan, 2001). It has since been shown that NS5 and the RdRp domain alone are capable of de novo synthesis using a poly(C) template, indicating that the MTase domain has little effect on the ability of the RdRp to perform this reaction (Selisko et al., 2006). HCV RdRp produced more abortive products than DENV RdRp in these experiments, consistent with the conformational change from initiation to elongation in HCV RdRp being more rate limiting (Selisko et al., 2006). Recently, it has been shown for DENV RdRp that the rate of formation of the elongation complex is temperature dependent; it occurs six times faster at 37 °C than at 30 °C (Jin et al., 2011). This agrees with the hypothesis that the DENV RdRp undergoes a conformational change from a 'closed' initiation complex to an 'open' elongation complex.

Many structures of viral RdRps have been determined, including members of all three genera of the family *Flaviviridae*. Several structures of HCV RdRp, and the RdRp from Bovine diarrhea virus (BVDV), a member of the genus pestivirus, have been solved (Choi et al., 2004; Lesburg et al., 1999; Ago et al., 1999). Also structures of the flavivirus polymerases from WNV and DENV have been determined (Malet et al., 2007; Yap et al., 2007). The polymerases from hepaciviruses, pestiviruses, and flaviviruses have low sequence homology (about 15% amino-acid identity), and significant structural diversity since it was not possible to determine the structures of the flavivirus polymerases by molecular replacement using the structures of the HCV or BVDV RdRps (Malet et al., 2007). However, they have several features in common. In addition, primer-independent RdRps share several sequence motifs (A–G) that are predicted to have specific roles in substrate binding and catalysis (Bruenn, 2003; Koonin, 1991). All the RdRp structures from viruses within the family *Flaviviridae* have a typical right-handed polymerase architecture (also seen in DNA polymerases) consisting of fingers, palm, and thumb subdomains. Unlike the DNA polymerases, flavivirus RdRps have a link at the top of the molecule between the fingers and thumb subdomains so that the active site is fully encircled by the enzyme (Lesburg et al., 1999; Ago et al., 1999). As a result, flavivirus polymerases have a more 'closed' conformation and less flexibility than other polymerases (Ferrer-Orta et al., 2006).

The DENV and WNV polymerases adopt very similar folds with root-mean-square deviations (RMSD) between the fingers, palm and thumb subdomains of 1.9, 0.8, and 1.0 Å, respectively (Malet et al., 2008). Both structures are thought to be the 'closed' conformation of the enzyme that is required for initiation of RNA synthesis. The WNV polymerase structure is slightly more open with the fingers subdomain rotated about 8° towards the thumb (Yap et al., 2007). Both polymerase structures contain two tunnels. One tunnel is down the fingers subdomain and this is thought to allow a path for the single-stranded RNA template (Malet et al., 2008; Yap et al., 2007). The second tunnel is through the center of the protein and this is thought to provide a route for the entry of NTPs to the active site.

The DENV RdRp contains two functional nuclear-localization sequences (NLS) (Brooks et al., 2002). DENV-2 NS5 has been shown to enter the nucleus, whereas WNV NS5 does not (Malet et al., 2007). The exact function of nucleus localization of DENV NS5 remains to be determined. However, mutagenesis of conserved residues that prevent NS5 localization to the nucleus, also blocks viral replication (Pryor et al., 2007). The βNLS includes three short helices on the surface of the thumb subdomain and the α/βNLS is on helices 6 and 7 and extends from the palm to the fingers subdomains.

The most conserved region of the polymerase is the palm and this is also structurally the most similar between WNV and DENV polymerases. This subdomain contains the active site motif GDD (part of motif C, residues 662–664 of DENV RdRp), which is at the tip of two β strands that are surrounded by eight α helices. The WNV and DENV RdRp structures were solved in the presence of Mg^{2+} ions. In both structures Mg^{2+} was coordinated between Asp664, part of motif C, and Asp 533 within motif A. The exact roles of metal ions in catalysis by the flavivirus polymerases are not clear. In vitro assays for the DENV RdRp require Mn^{2+} for activity (Yap et al., 2007; Niyomrattanakit et al., 2011), although Mg^{2+} is assumed to be the catalytic ion in vivo. In our unpublished data we have seen an Mn^{2+} ion bound between Asp663 and Asp533. This is in an equivalent position to one of the catalytic ions in the Φ6 RdRp structure with RNA and dNTPs (Butcher et al., 2001), indicating that this is the catalytically-relevant site.

The higher temperature factors in the crystal structure of DENV RdRp indicate that the fingers subdomain is the most mobile region in the polymerase (Yap et al., 2007). It contains a three-strand

β sheet that is not found in HCV or BVDV, as well as a region referred to as a fingertip because it reaches across the top of the enzyme into the thumb subdomain, encircling the active site. This fingertip includes the βNLS. Motif F contributes to NTP binding in HCV and Φ6 polymerases (Bressanelli et al., 2002; Butcher et al., 2001); this motif in DENV RdRp is at the tip of α helix ten, far away from the active site. It is not clear what the role of this motif is in the flavivirus RdRps. For motif F to be involved in nucleotide binding, a complete reorganization of the fingers would be required. Flavivirus polymerases may have evolved a different mechanism of binding NTPs in the NTP tunnel for catalysis; experiments will be required to test this hypothesis.

The thumb subdomain is the most variable between different polymerases. In DENV RdRp, it consists of eight α helices that are in a different topology to that seen in HCV and BVDV RdRps (Ago et al., 1999; Choi et al., 2004; Lesburg et al., 1999; Yap et al., 2007). The thumb subdomain contains a priming loop (motif G, residues 782–809 in DENV) that enters into the active site cavity. It is held in place by intra-loop contacts and there is clear density for this entire loop in DENV RdRp, suggesting that it is not very mobile in the absence of RNA. This loop is not present in primer-dependent RdRps (Ferrer-Orta et al., 2006) and the equivalent loop in HCV has been shown to be essential for de novo RNA synthesis (Hong et al., 2001). The structure of Φ6 RdRp in complex with single-stranded RNA and NTP showed that a conserved Tyr residue in the priming loop stacks against the base of the incoming NTP. This Tyr is conserved in HCV, but not in flavivirus RdRps. Instead these polymerases contain a Trp (position 795 in DENV RdRp) that may perform the same role (Malet et al., 2008; Yap et al., 2007).

The structure of the DENV polymerase was also determined in complex with rGTP (Yap et al., 2007). In the crystal-soaking conditions, the Mg^{2+} ion was lost, but electron density was seen for the three phosphates of the GTP. The triphosphates of GTP are bound to the three conserved residues (Ser710, Arg729, and Arg737); the GTP is approximately 7 Å from the catalytic GDD motif; and the guanosine base of GTP is in the correct position to stack against Trp795 during priming. Mutagenesis of the equivalent residues of the Ser and the first Arg in BVDV (both part of motif E) lead to a modest reduction in elongation activity, but a more significant effect on de novo activity (Lai et al., 1999), indicating that binding of the NTP at this site is required during initiation for de novo RNA synthesis. A high concentration of GTP is required by DENV polymerase for de novo RNA synthesis, even when GTP is not required as a substrate for initiation, suggesting that GTP is important for the initiation conformation (Nomaguchi et al., 2003).

Models for WNV and DENV RdRp bound to a template RNA suggest that there would be a few steric clashes for binding a single-stranded template RNA to these conformations of the enzymes (Yap et al., 2007; Malet et al., 2008). By analogy to the Φ6 RdRp bound to template RNA and NTPs, a single strand of RNA was modeled on the putative RNA tunnel where it would be bound by electrostatic interactions, mainly to the fingers subdomain (Malet et al., 2008). It is likely that three NTP-binding sites are required for de novo RNA synthesis. The i site (initiation or priming site) binds the first nucleotide of the RNA chain; the i + 1 site (catalytic) is next to the catalytic GDD motif and binds the second nucleotide of the nascent chain. The structure of rGTP bound to BVDV indicates that there is another GTP binding site at the i − 1 site that mimics an additional nucleotide in a growing RNA strand; during de novo synthesis, this nucleotide is necessary to hold the 3′OH of the initiating nucleotide in place for nucleophilic attack on the α phosphate of the NTP in the catalytic site. It is likely that DENV RdRp also binds GTP at the i − 1 site during priming since de novo synthesis requires a high GTP concentration (Nomaguchi et al., 2003). After catalysis, the GTP is released, and the RNA and dinucleotide product move one nucleotide through the enzyme to the i − 1 site. After initiation, the polymerase has to undergo a conformational change to move the priming loop out of the center of the enzyme to accommodate double-stranded RNA during elongation.

DENV RdRp contains two structural Zn^{2+} atoms (Yap et al., 2007). Zn^{2+}-1 is co-ordinated by the conserved residues C446, C449, H441, and E437 within the fingers subdomain, while Zn^{2+}-2 is co-ordinated by H712, H714, C728, and C847 at the base of the thumb subdomain. The crystal structure of a shorter form of WNV RdRp that is enzymatically inactive contained the same two Zn^{2+} sites, whereas a structure of the longer, active enzyme contained Zn^{2+}-1 but had a disulphide instead of a Zn^{2+} ion bound to the Zn^{2+}-2 site (Malet et al., 2007). In the structure of the shorter WNV RdRp, the Zn^{2+}-2 site is co-ordinated by H717, T719, C733, and C852. One of the co-ordinating residues is Thr rather than His, which provides an O atom rather than N as the metal–ion ligand. It is likely that the affinity for the Zn^{2+} atom has been reduced; therefore, the Zn^{2+} atom may have been lost during purification. In the DENV polymerase structure, the Zn^{2+}-1 site also has oxygen co-ordination from the polymerase (E437), leading to a lower occupancy of Zn^{2+} in the crystal structure; this result again suggests that some of the Zn^{2+} ions had diffused away during the purification process.

An analysis of the surface of the DENV and WNV RdRps identified two conserved cavities on the surface of the enzymes that could potentially be targeted by small-molecule inhibitors (Malet et al., 2008). These cavities are both located within the thumb subdomain. Mutagenesis of residues within the larger of these cavities, cavity A, showed that only one residue (Lys756) affected DENV replication (Zou et al., 2011). However, when this mutation was engineered into the recombinant RdRp, it had no effect on RNA synthesis in vitro, suggesting that compounds that bind to this pocket would not be identified by high-throughput screening. The same analysis of cavity B showed that Leu328, Trp859, and Ile863 were essential for viral replication through affecting de novo RNA synthesis, indicating that this pocket could be targeted by rational design (Zou et al., 2011). However, it should be pointed out that this cavity is relatively small and may be difficult to discover a compound with high affinity to suppress viral replication.

HTS screening against HCV RdRp has identified a number of pockets that can be targeted for rational design and for which co-crystal structures are available. These can largely be summarized as palm I, palm II, thumb I and thumb II sites (Legrand-Abravanel et al., 2010). The equivalent pockets to those in the thumb subdomain of HCV polymerase have not been found in the flavivirus RdRps. However, a new crystal structure of DENV RdRp in complex with NITD-107 showed that the compound could bind in positions roughly equivalent to the palm site I and II in HCV RdRp (PDB ID 3VWS; Figs. 5 and 6). Although NITD-107 did not significantly inhibit RdRp activity (IC_{50} value of 110 μM), probably due to its low binding affinity to the enzyme, it opens the possibility of rational structure-based design of compounds targeting this site. One interesting feature of this co-crystal structure is the huge conformational change of the RdRp upon NITD-107 binding. Helix α5 becomes completely disordered, as do the fingertip loops 1 and 2 that encircle the active site. The compound also stabilizes the whole of loop 3 and an extra turn of helix α7. These changes may cause a large entropic penalty and hence explain the low affinity of the compounds. However, this is the first direct evidence for the huge conformational flexibility in this polymerase, and shows that the improved crystallization conditions can be used for rational design as well as in further experiments to understand the enzymology of the polymerase. HCV polymerase crystal structures have been used successfully in fragment-based optimization approaches (Antonysamy et al., 2008). A similar fragment-based strategy can now be followed for DENV RdRp.

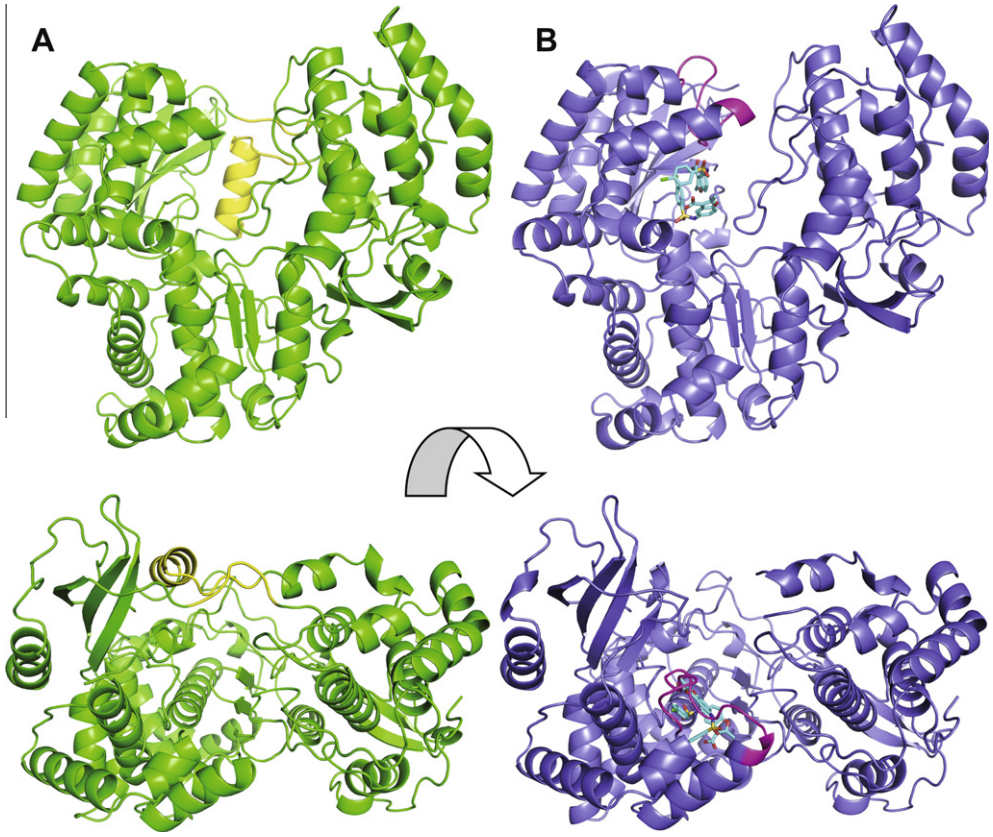

Fig. 5. Conformational changes in the crystal structure of the DENV RdRp. (A) 'Side' and 'top' views of the free DENV RdRp. (B) 'Side' and 'top' views of the DENV RdRp bound to two molecules of NITD-107 (PDB ID: 3VWS). The protein is shown as a cartoon and the compound molecules as sticks. The α helix and loops that become disordered upon compound binding are shown in yellow; the loop and helical turn that are stabilized by the compounds are shown in pink.

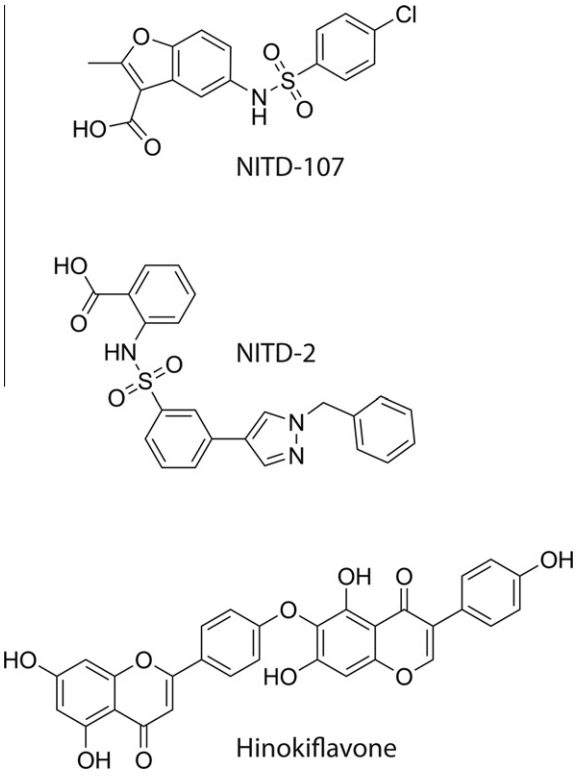

Fig. 6. Structures of compounds that inhibit or bind to the DENV RdRp in vitro.

Compounds that bind to the free form of the HCV polymerase exhibit multiple modes of inhibition. For example, compounds that bind to the thumb II site typically block conformational changes required for the transition from initiation to elongation (Biswal et al., 2005; Di et al., 2005; Howe et al., 2006). The conformation of the HCV polymerase in the crystal structures are thought to represent the 'closed' conformation required for de novo initiation of RNA synthesis so compounds that bind to these structures are more likely to inhibit initiation. Compounds that bind to the palm pocket have also been shown to inhibit initiation but not elongation (Gu et al., 2003; Liu et al., 2006). Some compounds that bind in crystal structures also inhibit elongation, for example if they are interfering with nucleotide incorporation (Reich et al., 2010; Powdrill et al., 2010). Recently, the crystal structure of HCV RdRp in complex with double-stranded RNA was determined (Mosley et al., 2012). This structure was captured by removing the priming β hairpin containing motif G and thereby opening up the central cavity to allow double-stranded RNA to bind. It may be possible to use this structure and approach for rational design of inhibitors that bind to the enzyme–RNA complex, since the enzyme is still active and is inhibited by chain-terminator compounds (Mosley et al., 2012). Compounds that bind to the enzyme-RNA complex would be expected to inhibit elongation.

Sulfonylanthranilic acid compounds (Fig. 6) were reported to bind to DENV RdRp in an allosteric site similar to the palm I site in HCV and compete with RNA binding (Niyomrattanakit et al., 2010; Yin et al., 2009a). Co-crystallization did not show sufficient density for a model of the compound to be built, so the binding site was identified by UV-crosslinking and mass spectrometry. Other compounds targeting the DENV RdRp have been identified, including natural products from plant extracts (Allard et al., 2011;

Bourjot et al., 2012; Coulerie et al., 2012). The most potent of these were biflavonoids that had sub-micromolar activity on DENV RdRp, but were inactive against the related BVDV and HCV RdRps (Coulerie et al., 2012). The mechanism of these compounds has yet to be explored. To date there are no compounds that inhibit DENV RdRp in vitro that have shown potent activity in cell-based assays.

5. Conclusions

The success of anti-DENV drug discovery relies on the understanding of viral replication at a molecular level. The availability of structural information about key enzymes involved in viral replication has provided a solid foundation for rational design as well as for HTS to identify antiviral compounds. Due to the similarity between HCV and DENV, the HCV strategies should be applicable to DENV drug discovery. Among the three enzymes reviewed in this communication, inhibitors of HCV protease have already been approved for clinical use, and inhibitors of HCV RdRp are in late clinical trials. Since dengue is an acute disease, treatment duration of dengue patients is expected to be less than a week. Therefore, the toxicity hurdle for the development of dengue therapies should be lower than that for HCV treatments (a chronic disease).

The DENV helicase has been largely ignored as a drug target, partly because of the difficulty in establishing a robust high-throughput assay and partly through learning from HCV, where no clinical candidates have emerged. However DENV helicase is inhibited in vitro by the natural product, Ivermectin (Mastrangelo et al., 2012). This compound was identified through *in silico* docking and was predicted to interact with residues including Thr408 and Asp409. Site-directed mutagenesis of these residues produced helicases that are resistant to inhibition by Ivermectin, suggesting that Ivermectin is a specific inhibitor of the flavivirus helicase. Ivermectin was also shown to be potent in cell culture, so it will be interesting to see if the compound shows efficacy in vivo.

Besides direct-acting antiviral approaches, two alternative approaches could be pursued for treatment of DENV-infected patients. The first is to identify compounds that inhibit host factors that are essential for viral replication. This approach has been successful in the discovery of the CCR5 antagonist that is in clinical use for the treatment of HIV (Emmelkamp and Rockstroh, 2007) (CCR5 is one of the co-receptors for HIV entry). The challenge of this approach is selectivity since host factors may have other unknown functions. If these are inhibited, it may lead to unpredicted toxicity. The second alternative approach is to identify compounds that inhibit the pathological pathway that leads to severe dengue disease. However, the feasibility of this approach suffers from the lack of knowledge of the molecular details of the disease pathology. More studies on the pathogenesis of DHF and DSS are needed before this approach can be rationally pursued.

Among the three approaches discussed above, the direct-acting antiviral represents the most straightforward approach to deliver clinical candidates for dengue therapy. However, when direct-acting antivirals become available, it remains to be proved that suppression of viraemia can prevent infected patients from developing severe dengue. Despite all these potential challenges, we should continue a concerted effort towards the development of anti-dengue therapeutics.

Acknowledgements

We thank Julien Lescar, Siew Pheng Lim, Qing-Yin Wang, Yen-Liang Chen, and Hongping Dong for helpful discussions, and Siew Pheng Lim for reading through the manuscript.

References

Ackermann, M., Padmanabhan, R., 2001. De novo synthesis of RNA by the dengue virus RNA-dependent RNA polymerase exhibits temperature dependence at the initiation but not elongation phase. J. Biol. Chem. 276, 39926–39937.

Ago, H., Adachi, T., Yoshida, A., Yamamoto, M., Habuka, N., Yatsunami, K., Miyano, M., 1999. Crystal structure of the RNA-dependent RNA polymerase of hepatitis C virus. Structure 7, 1417–1426.

Aleshin, A.E., Shiryaev, S.A., Strongin, A.Y., Liddington, R.C., 2007. Structural evidence for regulation and specificity of flaviviral proteases and evolution of the Flaviviridae fold. Protein Sci. 16, 795–806.

Allard, P.M., Dau, E.T., Eydoux, C., Guillemot, J.C., Dumontet, V., Poullain, C., Canard, B., Gueritte, F., Litaudon, M., 2011. Alkylated flavanones from the bark of *Cryptocarya chartacea* as dengue virus NS5 polymerase inhibitors. J. Nat. Prod. 74, 2446–2453.

Antonysamy, S.S., Aubol, B., Blaney, J., Browner, M.F., Giannetti, A.M., Harris, S.F., Hebert, N., Hendle, J., Hopkins, S., Jefferson, E., Kissinger, C., Leveque, V., Marciano, D., McGee, E., Najera, I., Nolan, B., Tomimoto, M., Torres, E., Wright, T., 2008. Fragment-based discovery of hepatitis C virus NS5b RNA polymerase inhibitors. Bioorg. Med. Chem. Lett. 18, 2990–2995.

Assenberg, R., Mastrangelo, E., Walter, T.S., Verma, A., Milani, M., Owens, R.J., Stuart, D.I., Grimes, J.M., Mancini, E.J., 2009. Crystal structure of a novel conformational state of the flavivirus NS3 protein: implications for polyprotein processing and viral replication. J. Virol. 83, 12895–12906.

Assenberg, R., Ren, J., Verma, A., Walter, T.S., Alderton, D., Hurrelbrink, R.J., Fuller, S.D., Bressanelli, S., Owens, R.J., Stuart, D.I., Grimes, J.M., 2007. Crystal structure of the Murray Valley encephalitis virus NS5 methyltransferase domain in complex with cap analogues. J. Gen. Virol. 88, 2228–2236.

Benarroch, D., Egloff, M.P., Mulard, L., Guerreiro, C., Romette, J.L., Canard, B., 2004. A structural basis for the inhibition of the NS5 dengue virus mRNA 2′-O-methyltransferase domain by ribavirin 5′-triphosphate. J. Biol. Chem. 279, 35638–35643.

Biswal, B.K., Cherney, M.M., Wang, M., Chan, L., Yannopoulos, C.G., Bilimoria, D., Nicolas, O., Bedard, J., James, M.N., 2005. Crystal structures of the RNA-dependent RNA polymerase genotype 2a of hepatitis C virus reveal two conformations and suggest mechanisms of inhibition by non-nucleoside inhibitors. J. Biol. Chem. 280, 18202–18210.

Bodenreider, C., Beer, D., Keller, T.H., Sonntag, S., Wen, D., Yap, L., Yau, Y.H., Shochat, S.G., Huang, D., Zhou, T., Caflisch, A., Su, X.C., Ozawa, K., Otting, G., Vasudevan, S.G., Lescar, J., Lim, S.P., 2009. A fluorescence quenching assay to discriminate between specific and nonspecific inhibitors of dengue virus protease. Anal. Biochem. 395, 195–204.

Bollati, M., Alvarez, K., Assenberg, R., Baronti, C., Canard, B., Cook, S., Coutard, B., Decroly, E., de Lamballerie, X., Gould, E.A., Grard, G., Grimes, J.M., Hilgenfeld, R., Jansson, A.M., Malet, H., Mancini, E.J., Mastrangelo, E., Mattevi, A., Milani, M., Moureau, G., Neyts, J., Owens, R.J., Ren, J., Selisko, B., Speroni, S., Steuber, H., Stuart, D.I., Unge, T., Bolognesi, M., 2010. Structure and functionality in flavivirus NS-proteins: perspectives for drug design. Antiviral Res. 87, 125–148.

Bollati, M., Milani, M., Mastrangelo, E., Ricagno, S., Tedeschi, G., Nonnis, S., Decroly, E., Selisko, B., de Lamballerie, X., Coutard, B., Canard, B., Bolognesi, M., 2009. Recognition of RNA cap in the Wesselsbron virus NS5 methyltransferase domain: implications for RNA-capping mechanisms in flavivirus. J. Mol. Biol. 385, 140–152.

Bourjot, M., Leyssen, P., Eydoux, C., Guillemot, J.C., Canard, B., Rasoanaivo, P., Gueritte, F., Litaudon, M., 2012. Flacourtosides A–F, phenolic glycosides isolated from flacourtia ramontchi. J. Nat. Prod. 75, 752–758.

Bressanelli, S., Tomei, L., Rey, F.A., De, F.R., 2002. Structural analysis of the hepatitis C virus RNA polymerase in complex with ribonucleotides. J. Virol. 76, 3482–3492.

Brooks, A.J., Johansson, M., John, A.V., Xu, Y., Jans, D.A., Vasudevan, S.G., 2002. The interdomain region of dengue NS5 protein that binds to the viral helicase NS3 contains independently functional importin beta 1 and importin alpha/beta-recognized nuclear localization signals. J. Biol. Chem. 277, 36399–36407.

Bruenn, J.A., 2003. A structural and primary sequence comparison of the viral RNA-dependent RNA polymerases. Nucleic Acids Res. 31, 1821–1829.

Butcher, S.J., Grimes, J.M., Makeyev, E.V., Bamford, D.H., Stuart, D.I., 2001. A mechanism for initiating RNA-dependent RNA polymerization. Nature 410, 235–240.

Chandramouli, S., Joseph, J.S., Daudenarde, S., Gatchalian, J., Cornillez-Ty, C., Kuhn, P., 2010. Serotype-specific structural differences in the protease-cofactor complexes of the dengue virus family. J. Virol. 84, 3059–3067.

Chappell, K.J., Stoermer, M.J., Fairlie, D.P., Young, P.R., 2006. Insights to substrate binding and processing by West Nile Virus NS3 protease through combined modeling, protease mutagenesis, and kinetic studies. J. Biol. Chem. 281, 38448–38458.

Choi, K.H., Groarke, J.M., Young, D.C., Kuhn, R.J., Smith, J.L., Pevear, D.C., Rossmann, M.G., 2004. The structure of the RNA-dependent RNA polymerase from bovine viral diarrhea virus establishes the role of GTP in de novo initiation. Proc. Natl. Acad. Sci. USA 101, 4425–4430.

Chu, P.W., Westaway, E.G., 1985. Replication strategy of Kunjin virus: evidence for recycling role of replicative form RNA as template in semiconservative and asymmetric replication. Virology 140, 68–79.

Coulerie, P., Eydoux, C., Hnawia, E., Stuhl, L., Maciuk, A., Lebouvier, N., Canard, B., Figadere, B., Guillemot, J.C., Nour, M., 2012. Biflavonoids of *Dacrydium balansae*

with potent inhibitory activity on dengue 2 NS5 polymerase. Planta Med. 78, 672–677.
Daffis, S., Szretter, K.J., Schriewer, J., Li, J., Youn, S., Errett, J., Lin, T.Y., Schneller, S., Zust, R., Dong, H., Thiel, V., Sen, G.C., Fensterl, V., Klimstra, W.B., Pierson, T.C., Buller, R.M., Gale Jr., M., Shi, P.Y., Diamond, M.S., 2010. 2′-O methylation of the viral mRNA cap evades host restriction by IFIT family members. Nature 468, 452–456.
de la Cruz, L., Nguyen, T.H., Ozawa, K., Shin, J., Graham, B., Huber, T., Otting, G., 2011. Binding of low molecular weight inhibitors promotes large conformational changes in the dengue virus NS2B–NS3 protease: fold analysis by pseudocontact shifts. J. Am. Chem. Soc. 133, 19205–19215.
Di, M.S., Volpari, C., Tomei, L., Altamura, S., Harper, S., Narjes, F., Koch, U., Rowley, M., De, F.R., Migliaccio, G., Carfi, A., 2005. Interdomain communication in hepatitis C virus polymerase abolished by small molecule inhibitors bound to a novel allosteric site. J. Biol. Chem. 280, 29765–29770.
Dong, H., Chang, D.C., Hua, M.H., Lim, S.P., Chionh, Y.H., Hia, F., Lee, Y.H., Kukkaro, P., Lok, S.M., Dedon, P.C., Shi, P.Y., 2012. 2′-O methylation of internal adenosine by flavivirus NS5 methyltransferase. PLoS Pathog. 8, e1002642.
Dong, H., Chang, D.C., Xie, X., Toh, Y.X., Chung, K.Y., Zou, G., Lescar, J., Lim, S.P., Shi, P.Y., 2010a. Biochemical and genetic characterization of dengue virus methyltransferase. Virology 405, 568–578.
Dong, H., Liu, L., Zou, G., Zhao, Y., Li, Z., Lim, S.P., Shi, P.Y., Li, H., 2010b. Structural and functional analyses of a conserved hydrophobic pocket of flavivirus methyltransferase. J. Biol. Chem. 285, 32586–32595.
Dong, H., Ray, D., Ren, S., Zhang, B., Puig-Basagoiti, F., Takagi, Y., Ho, C.K., Li, H., Shi, P.Y., 2007. Distinct RNA elements confer specificity to flavivirus RNA cap methylation events. J. Virol. 81, 4412–4421.
Dong, H., Ren, S., Zhang, B., Zhou, Y., Puig-Basagoiti, F., Li, H., Shi, P.Y., 2008a. West Nile virus methyltransferase catalyzes two methylations of the viral RNA cap through a substrate-repositioning mechanism. J. Virol. 82, 4295–4307.
Dong, H., Zhang, B., Shi, P.Y., 2008b. Flavivirus methyltransferase: a novel antiviral target. Antiviral Res. 80, 1–10.
Egloff, M.P., Benarroch, D., Selisko, B., Romette, J.L., Canard, B., 2002. An RNA cap (nucleoside-2′-O-)-methyltransferase in the flavivirus RNA polymerase NS5: crystal structure and functional characterization. EMBO J. 21, 2757–2768.
Egloff, M.P., Decroly, E., Malet, H., Selisko, B., Benarroch, D., Ferron, F., Canard, B., 2007. Structural and functional analysis of methylation and 5′-RNA sequence requirements of short capped RNAs by the methyltransferase domain of dengue virus NS5. J. Mol. Biol. 372, 723–736.
Emmelkamp, J.M., Rockstroh, J.K., 2007. CCR5 antagonists: comparison of efficacy, side effects, pharmacokinetics and interactions – review of the literature. Eur. J. Med. Res. 12, 409–417.
Erbel, P., Schiering, N., D'Arcy, A., Renatus, M., Kroemer, M., Lim, S.P., Yin, Z., Keller, T.H., Vasudevan, S.G., Hommel, U., 2006. Structural basis for the activation of flaviviral NS3 proteases from dengue and West Nile virus. Nat. Struct. Mol. Biol. 13, 372–373.
Falgout, B., Pethel, M., Zhang, Y.M., Lai, C.J., 1991. Both nonstructural proteins NS2B and NS3 are required for the proteolytic processing of dengue virus nonstructural proteins. J. Virol. 65, 2467–2475.
Ferrer-Orta, C., Arias, A., Escarmis, C., Verdaguer, N., 2006. A comparison of viral RNA-dependent RNA polymerases. Curr. Opin. Struct. Biol. 16, 27–34.
Geiss, B.J., Stahla-Beek, H.J., Hannah, A.M., Gari, H.H., Henderson, B.R., Saeedi, B.J., Keenan, S.M., 2011. A high-throughput screening assay for the identification of flavivirus NS5 capping enzyme GTP-binding inhibitors: implications for antiviral drug development. J. Biomol. Screen. 16, 852–861.
Geiss, B.J., Thompson, A.A., Andrews, A.J., Sons, R.L., Gari, H.H., Keenan, S.M., Peersen, O.B., 2009. Analysis of flavivirus NS5 methyltransferase cap binding. J. Mol. Biol. 385, 1643–1654.
Ghosh, A., Lima, C.D., 2010. Enzymology of RNA cap synthesis. WIREs RNA 1, 152–172.
Gu, B., Johnston, V.K., Gutshall, L.L., Nguyen, T.T., Gontarek, R.R., Darcy, M.G., Tedesco, R., Dhanak, D., Duffy, K.J., Kao, C.C., Sarisky, R.T., 2003. Arresting initiation of hepatitis C virus RNA synthesis using heterocyclic derivatives. J. Biol. Chem. 278, 16602–16607.
Hong, Z., Cameron, C.E., Walker, M.P., Castro, C., Yao, N., Lau, J.Y., Zhong, W., 2001. A novel mechanism to ensure terminal initiation by hepatitis C virus NS5B polymerase. Virology 285, 6–11.
Howe, A.Y., Cheng, H., Thompson, I., Chunduru, S.K., Herrmann, S., O'Connell, J., Agarwal, A., Chopra, R., Del Vecchio, A.M., 2006. Molecular mechanism of a thumb domain hepatitis C virus nonnucleoside RNA-dependent RNA polymerase inhibitor. Antimicrob. Agents Chemother. 50, 4103–4113.
Issur, M., Geiss, B.J., Bougie, I., Picard-Jean, F., Despins, S., Mayette, J., Hobdey, S.E., Bisaillon, M., 2009. The flavivirus NS5 protein is a true RNA guanylyltransferase that catalyzes a two-step reaction to form the RNA cap structure. RNA 15, 2340–2350.
Jansson, A.M., Jakobsson, E., Johansson, P., Lantez, V., Coutard, B., de Lamballerie, X., Unge, T., Jones, T.A., 2009. Structure of the methyltransferase domain from the Modoc virus, a flavivirus with no known vector. Acta Crystallogr. D Biol. Crystallogr. 65, 796–803.
Jin, Z., Deval, J., Johnson, K.A., Swinney, D.C., 2011. Characterization of the elongation complex of dengue virus RNA polymerase: assembly, kinetics of nucleotide incorporation, and fidelity. J. Biol. Chem. 286, 2067–2077.
Knehans, T., Schuller, A., Doan, D.N., Nacro, K., Hill, J., Guntert, P., Madhusudhan, M.S., Weil, T., Vasudevan, S.G., 2011. Structure-guided fragment-based in silico drug design of dengue protease inhibitors. J. Comput. Aided Mol. Des. 25, 263–274.
Koonin, E.V., 1991. The phylogeny of RNA-dependent RNA polymerases of positive-strand RNA viruses. J. Gen. Virol. 72 (Pt 9), 2197–2206.
Lai, V.C., Kao, C.C., Ferrari, E., Park, J., Uss, A.S., Wright-Minogue, J., Hong, Z., Lau, J.Y., 1999. Mutational analysis of bovine viral diarrhea virus RNA-dependent RNA polymerase. J. Virol. 73, 10129–10136.
Legrand-Abravanel, F., Nicot, F., Izopet, J., 2010. New NS5B polymerase inhibitors for hepatitis C. Expert Opin. Investig. Drugs 19, 963–975.
Lesburg, C.A., Cable, M.B., Ferrari, E., Hong, Z., Mannarino, A.F., Weber, P.C., 1999. Crystal structure of the RNA-dependent RNA polymerase from hepatitis C virus reveals a fully encircled active site. Nat. Struct. Biol. 6, 937–943.
Lescar, J., Luo, D., Xu, T., Sampath, A., Lim, S.P., Canard, B., Vasudevan, S.G., 2008. Towards the design of antiviral inhibitors against flaviviruses: the case for the multifunctional NS3 protein from dengue virus as a target. Antiviral Res. 80, 94–101.
Li, J., Lim, S.P., Beer, D., Patel, V., Wen, D., Tumanut, C., Tully, D.C., Williams, J.A., Jiricek, J., Priestle, J.P., Harris, J.L., Vasudevan, S.G., 2005. Functional profiling of recombinant NS3 proteases from all four serotypes of dengue virus using tetrapeptide and octapeptide substrate libraries. J. Biol. Chem. 280, 28766–28774.
Lim, S.P., Sonntag, L.S., Noble, C., Nilar, S.H., Ng, R.H., Zou, G., Monaghan, P., Chung, K.Y., Dong, H., Liu, B., Bodenreider, C., Lee, G., Ding, M., Chan, W.L., Wang, G., Jian, Y.L., Chao, A.T., Lescar, J., Yin, Z., Vedananda, T.R., Keller, T.H., Shi, P.Y., 2011. Small molecule inhibitors that selectively block dengue virus methyltransferase. J. Biol. Chem. 286, 6233–6240.
Lim, S.P., Wen, D., Yap, T.L., Yan, C.K., Lescar, J., Vasudevan, S.G., 2008. A scintillation proximity assay for dengue virus NS5 2′-O-methyltransferase-kinetic and inhibition analyses. Antiviral Res. 80, 360–369.
Liu, Y., Jiang, W.W., Pratt, J., Rockway, T., Harris, K., Vasavanonda, S., Tripathi, R., Pithawalla, R., Kati, W.M., 2006. Mechanistic study of HCV polymerase inhibitors at individual steps of the polymerization reaction. Biochemistry 45, 11312–11323.
Malet, H., Egloff, M.P., Selisko, B., Butcher, R.E., Wright, P.J., Roberts, M., Gruez, A., Sulzenbacher, G., Vonrhein, C., Bricogne, G., Mackenzie, J.M., Khromykh, A.A., Davidson, A.D., Canard, B., 2007. Crystal structure of the RNA polymerase domain of the West Nile virus non-structural protein 5. J. Biol. Chem. 282, 10678–10689.
Malet, H., Masse, N., Selisko, B., Romette, J.L., Alvarez, K., Guillemot, J.C., Tolou, H., Yap, T.L., Vasudevan, S., Lescar, J., Canard, B., 2008. The flavivirus polymerase as a target for drug discovery. Antiviral Res. 80, 23–35.
Mastrangelo, E., Pezzullo, M., De, B.T., Kaptein, S., Pastorino, B., Dallmeier, K., de Lamballerie, X., Neyts, J., Hanson, A.M., Frick, D.N., Bolognesi, M., Milani, M., 2012. Ivermectin is a potent inhibitor of flavivirus replication specifically targeting NS3 helicase activity: new prospects for an old drug. J. Antimicrob. Chemother. 67, 1884–1894.
Milani, M., Mastrangelo, E., Bollati, M., Selisko, B., Decroly, E., Bouvet, M., Canard, B., Bolognesi, M., 2009. Flaviviral methyltransferase/RNA interaction: structural basis for enzyme inhibition. Antiviral Res. 83, 28–34.
Mosley, R.T., Edwards, T.E., Murakami, E., Lam, A.M., Grice, R.L., Du, J., Sofia, M.J., Furman, P.A., Otto, M.J., 2012. Structure of HCV polymerase in complex with primer-template RNA. J. Virol. 86, 6503–6511.
Mueller, N.H., Yon, C., Ganesh, V.K., Padmanabhan, R., 2007. Characterization of the West Nile virus protease substrate specificity and inhibitors. Int. J. Biochem. Cell Biol. 39, 606–614.
Nitsche, C., Behnam, M.A., Steuer, C., Klein, C.D., 2012. Retro peptide-hybrids as selective inhibitors of the dengue virus NS2B–NS3 protease. Antiviral Res. 94, 72–79.
Niyomrattanakit, P., Abas, S.N., Lim, C.C., Beer, D., Shi, P.Y., Chen, Y.L., 2011. A fluorescence-based alkaline phosphatase-coupled polymerase assay for identification of inhibitors of dengue virus RNA-dependent RNA polymerase. J. Biomol. Screen. 16, 201–210.
Niyomrattanakit, P., Chen, Y.L., Dong, H., Yin, Z., Qing, M., Glickman, J.F., Lin, K., Mueller, D., Voshol, H., Lim, J.Y., Nilar, S., Keller, T.H., Shi, P.Y., 2010. Inhibition of dengue virus polymerase by blocking of the RNA tunnel. J. Virol. 84, 5678–5686.
Noble, C.G., Chen, Y.L., Dong, H., Gu, F., Lim, S.P., Schul, W., Wang, Q.Y., Shi, P.Y., 2010. Strategies for development of dengue virus inhibitors. Antiviral Res. 85, 450–462.
Noble, C.G., Seh, C.C., Chao, A.T., Shi, P.Y., 2012. Ligand-bound structures of the dengue virus protease reveal the active conformation. J. Virol. 86, 438–446.
Nomaguchi, M., Ackermann, M., Yon, C., You, S., Padmanabhan, R., 2003. De novo synthesis of negative-strand RNA by dengue virus RNA-dependent RNA polymerase in vitro: nucleotide, primer, and template parameters. J. Virol. 77, 8831–8842.
Powdrill, M.H., Deval, J., Narjes, F., De, F.R., Gotte, M., 2010. Mechanism of hepatitis C virus RNA polymerase inhibition with dihydroxypyrimidines. Antimicrob. Agents Chemother. 54, 977–983.
Pryor, M.J., Rawlinson, S.M., Butcher, R.E., Barton, C.L., Waterhouse, T.A., Vasudevan, S.G., Bardin, P.G., Wright, P.J., Jans, D.A., Davidson, A.D., 2007. Nuclear localization of dengue virus nonstructural protein 5 through its importin alpha/beta-recognized nuclear localization sequences is integral to viral infection. Traffic 8, 795–807.
Rawlinson, S.M., Pryor, M.J., Wright, P.J., Jans, D.A., 2006. Dengue virus RNA polymerase NS5: a potential therapeutic target? Curr. Drug Targets 7, 1623–1638.
Ray, D., Shah, A., Tilgner, M., Guo, Y., Zhao, Y., Dong, H., Deas, T.S., Zhou, Y., Li, H., Shi, P.Y., 2006. West Nile virus 5′-cap structure is formed by sequential guanine N-7

and ribose 2′-O methylations by nonstructural protein 5. J. Virol. 80, 8362–8370.
Reich, S., Golbik, R.P., Geissler, R., Lilie, H., Behrens, S.E., 2010. Mechanisms of activity and inhibition of the hepatitis C virus RNA-dependent RNA polymerase. J. Biol. Chem. 285, 13685–13693.
Robin, G., Chappell, K., Stoermer, M.J., Hu, S.H., Young, P.R., Fairlie, D.P., Martin, J.L., 2009. Structure of West Nile virus NS3 protease: ligand stabilization of the catalytic conformation. J. Mol. Biol. 385, 1568–1577.
Schuller, A., Yin, Z., Brian Chia, C.S., Doan, D.N., Kim, H.K., Shang, L., Loh, T.P., Hill, J., Vasudevan, S.G., 2011. Tripeptide inhibitors of dengue and West Nile virus NS2B–NS3 protease. Antiviral Res. 92, 96–101.
Selisko, B., Dutartre, H., Guillemot, J.C., Debarnot, C., Benarroch, D., Khromykh, A., Despres, P., Egloff, M.P., Canard, B., 2006. Comparative mechanistic studies of de novo RNA synthesis by flavivirus RNA-dependent RNA polymerases. Virology 351, 145–158.
Shiryaev, S.A., Kozlov, I.A., Ratnikov, B.I., Smith, J.W., Lebl, M., Strongin, A.Y., 2007a. Cleavage preference distinguishes the two-component NS2B–NS3 serine proteinases of dengue and West Nile viruses. Biochem. J. 401, 743–752.
Shiryaev, S.A., Ratnikov, B.I., Aleshin, A.E., Kozlov, I.A., Nelson, N.A., Lebl, M., Smith, J.W., Liddington, R.C., Strongin, A.Y., 2007b. Switching the substrate specificity of the two-component NS2B–NS3 flavivirus proteinase by structure-based mutagenesis. J. Virol. 81, 4501–4509.
Simmons, C.P., Farrar, J.J., Nguyen, V., Wills, B., 2012. Dengue. N. Engl. J. Med. 366, 1423–1432.
Stahla-Beek, H.J., April, D.G., Saeedi, B.J., Hannah, A.M., Keenan, S.M., Geiss, B.J., 2012. Identification of a novel antiviral inhibitor of the flavivirus guanylyltransferase enzyme. J. Virol. 86, 8730–8739.
Stoermer, M.J., Chappell, K.J., Liebscher, S., Jensen, C.M., Gan, C.H., Gupta, P.K., Xu, W.J., Young, P.R., Fairlie, D.P., 2008. Potent cationic inhibitors of West Nile virus NS2B/NS3 protease with serum stability, cell permeability and antiviral activity. J. Med. Chem. 51, 5714–5721.
Su, X.C., Ozawa, K., Qi, R., Vasudevan, S.G., Lim, S.P., Otting, G., 2009. NMR analysis of the dynamic exchange of the NS2B cofactor between open and closed conformations of the West Nile virus NS2B–NS3 protease. PLoS Negl. Trop. Dis. 3, e561.
Tomlinson, S.M., Malmstrom, R.D., Russo, A., Mueller, N., Pang, Y.P., Watowich, S.J., 2009. Structure-based discovery of dengue virus protease inhibitors. Antiviral Res. 82, 110–114.
Tomlinson, S.M., Watowich, S.J., 2012. Use of parallel validation high-throughput screens to reduce false positives and identify novel dengue NS2B–NS3 protease inhibitors. Antiviral Res. 93, 245–252.
Valle, R.P., Falgout, B., 1998. Mutagenesis of the NS3 protease of dengue virus type 2. J. Virol. 72, 624–632.
Venkatraman, S., 2012. Discovery of boceprevir, a direct-acting NS3/4A protease inhibitor for treatment of chronic hepatitis C infections. Trends Pharmacol. Sci. 33, 289–294.
Wengler, G., Castle, E., Leidner, U., Nowak, T., Wengler, G., 1985. Sequence analysis of the membrane protein V3 of the flavivirus West Nile virus and of its gene. Virology 147, 264–274.
Wichapong, K., Pianwanit, S., Sippl, W., Kokpol, S., 2010. Homology modeling and molecular dynamics simulations of dengue virus NS2B/NS3 protease: insight into molecular interaction. J. Mol. Recognit. 23, 283–300.
Wu, P.S.C., Ozawa, K., Lim, S.P., Vasudevan, S.G., Dixon, N.E., Otting, G., 2007. Cell-free transcription/translation from PCR-amplified DNA for high-throughput NMR studies. Angew. Chem. Int. Ed. 46, 3356–3358.
Xie, X., Wang, Q.Y., Xu, H.Y., Qing, M., Kramer, L., Yuan, Z., Shi, P.Y., 2011. Inhibition of dengue virus by targeting viral NS4B protein. J. Virol. 85, 11183–11195.
Yap, L.J., Luo, D., Chung, K.Y., Lim, S.P., Bodenreider, C., Noble, C., Shi, P.Y., Lescar, J., 2010. Crystal structure of the dengue virus methyltransferase bound to a 5′-capped octameric RNA. PLoS ONE 5, e12836.
Yap, T.L., Xu, T., Chen, Y.L., Malet, H., Egloff, M.P., Canard, B., Vasudevan, S.G., Lescar, J., 2007. Crystal structure of the dengue virus RNA-dependent RNA polymerase catalytic domain at 1.85-angstrom resolution. J. Virol. 81, 4753–4765.
Yin, Z., Chen, Y.L., Kondreddi, R.R., Chan, W.L., Wang, G., Ng, R.H., Lim, J.Y., Lee, W.Y., Jeyaraj, D.A., Niyomrattanakit, P., Wen, D., Chao, A., Glickman, J.F., Voshol, H., Mueller, D., Spanka, C., Dressler, S., Nilar, S., Vasudevan, S.G., Shi, P.Y., Keller, T.H., 2009a. N-sulfonylanthranilic acid derivatives as allosteric inhibitors of dengue viral RNA-dependent RNA polymerase. J. Med. Chem. 52, 7934–7937.
Yin, Z., Chen, Y.L., Schul, W., Wang, Q.Y., Gu, F., Duraiswamy, J., Kondreddi, R.R., Niyomrattanakit, P., Lakshminarayana, S.B., Goh, A., Xu, H.Y., Liu, W., Liu, B., Lim, J.Y., Ng, C.Y., Qing, M., Lim, C.C., Yip, A., Wang, G., Chan, W.L., Tan, H.P., Lin, K., Zhang, B., Zou, G., Bernard, K.A., Garrett, C., Beltz, K., Dong, M., Weaver, M., He, H., Pichota, A., Dartois, V., Keller, T.H., Shi, P.Y., 2009b. An adenosine nucleoside inhibitor of dengue virus. Proc. Natl. Acad. Sci. USA 106, 20435–20439.
Yin, Z., Patel, S.J., Wang, W.L., Chan, W.L., Ranga Rao, K.R., Wang, G., Ngew, X., Patel, V., Beer, D., Knox, J.E., Ma, N.L., Ehrhardt, C., Lim, S.P., Vasudevan, S.G., Keller, T.H., 2006a. Peptide inhibitors of dengue virus NS3 protease. Part 2: SAR study of tetrapeptide aldehyde inhibitors. Bioorg. Med. Chem. Lett. 16, 40–43.
Yin, Z., Patel, S.J., Wang, W.L., Wang, G., Chan, W.L., Rao, K.R., Alam, J., Jeyaraj, D.A., Ngew, X., Patel, V., Beer, D., Lim, S.P., Vasudevan, S.G., Keller, T.H., 2006b. Peptide inhibitors of dengue virus NS3 protease. Part 1: warhead. Bioorg. Med. Chem. Lett. 16, 36–39.
You, S., Padmanabhan, R., 1999. A novel in vitro replication system for dengue virus. Initiation of RNA synthesis at the 3′-end of exogenous viral RNA templates requires 5′- and 3′-terminal complementary sequence motifs of the viral RNA. J. Biol. Chem. 274, 33714–33722.
Zou, G., Chen, Y.L., Dong, H., Lim, C.C., Yap, L.J., Yau, Y.H., Shochat, S.G., Lescar, J., Shi, P.Y., 2011. Functional analysis of two cavities in flavivirus NS5 polymerase. J. Biol. Chem. 286, 14362–14372.